Poisson-Fermi modeling of ion activities in aqueous single and mixed electrolyte solutions at variable temperature

Jinn-Liang Liu, and Bob Eisenberg

Citation: The Journal of Chemical Physics **148**, 054501 (2018);
View online: https://doi.org/10.1063/1.5021508
View Table of Contents: http://aip.scitation.org/toc/jcp/148/5
Published by the American Institute of Physics

THE JOURNAL OF CHEMICAL PHYSICS **148**, 054501 (2018)
DOI: 10.1063/1.5021508

Poisson-Fermi modeling of ion activities in aqueous single and mixed electrolyte solutions at variable temperature

Jinn-Liang Liu[1,a)] and Bob Eisenberg[2,b)]
[1]*Institute of Computational and Modeling Science, National Tsing Hua University, Hsinchu 300, Taiwan*
[2]*Department of Physiology and Biophysics, Rush University, Chicago, Illinois 60612, USA and Department of Applied Mathematics, Illinois Institute of Technology, Chicago, Illinois 60616, USA*

(Received 4 January 2018; accepted 13 January 2018; published online 1 February 2018)

The combinatorial explosion of empirical parameters in tens of thousands presents a tremendous challenge for extended Debye-Hückel models to calculate activity coefficients of aqueous mixtures of the most important salts in chemistry. The explosion of parameters originates from the phenomenological extension of the Debye-Hückel theory that does not take steric and correlation effects of ions and water into account. By contrast, the Poisson-Fermi theory developed in recent years treats ions and water molecules as nonuniform hard spheres of any size with interstitial voids and includes ion-water and ion-ion correlations. We present a Poisson-Fermi model and numerical methods for calculating the individual or mean activity coefficient of electrolyte solutions with any arbitrary number of ionic species in a large range of salt concentrations and temperatures. For each activity-concentration curve, we show that the Poisson-Fermi model requires only three unchanging parameters at most to well fit the corresponding experimental data. The three parameters are associated with the Born radius of the solvation energy of an ion in electrolyte solution that changes with salt concentrations in a highly nonlinear manner. *Published by AIP Publishing.* https://doi.org/10.1063/1.5021508

I. INTRODUCTION

Thermodynamic modeling of aqueous electrolyte solutions plays an important role in chemical and biological sciences.[1–13] Despite intense efforts in the past century, robust thermodynamic modeling of electrolyte solutions still presents a difficult challenge and remains a remote ambition in the extended Debye-Hückel (DH) models due to the enormous number of parameters that need to be adjusted, carefully and often subjectively.[11,13] For example, the Pitzer model requires 8 parameters for a ternary system and up to 8 temperature coefficients (parameters) for every Pitzer parameter in a temperature interval from 0 to about 200 °C.[11,13] It is indeed a frustrating despair (*frustration* on p. 11 in Ref. 9 and *despair* on p. 301 in Ref. 1) that approximately 22 000 parameters for combinatorial solutions of the most important 28 cations and 16 anions in salt chemistry have to be extracted from the available experimental data for one temperature.[11] The Pitzer model is still the most widely used DH model with unmatched precision for modeling aqueous electrolyte solutions over wide ranges of composition, temperature, and pressure.[13]

The Pitzer model and its variants[13] are all derived from the Debye-Hückel theory[14] that in turn is based on a linear Poisson-Boltzmann (PB) equation[5] although potentials calculated from PB near ions (for example) are often far beyond the linear range of the potential near ions or interfaces. The PB equation treats ions as point charges without steric volumes and water molecules as a homogeneous dielectric medium without steric volumes either and with a constant dielectric constant that neglects ion-water and ion-ion correlations. These simplifications give rise to the elegant, simple, and useful DH theory. However, it is precisely because of the linearization and simplifications on steric and correlation effects that extended DH models have needed an explosion in the number of parameters in order to overcome the deficiencies (simplifications) of the classical Poisson-Boltzmann theory. The nonlinear PB equation was developed by Gouy and Chapman.[15,16]

In the past few years, we have intensively investigated these two effects in a range of areas from electric double layers[17,18] and ion activities[19] to biological ion channels[18,20–24] and consequently developed an advanced theory—the Poisson-Fermi (PF) theory—that treats ions and water molecules as nonuniform hard spheres of any size with interstitial voids and includes many of the correlation effects of ions and water. We refer to our previous papers and references therein for a historical account of the literature of this theory. In Ref. 19, we proposed a PF model for calculating activity coefficients of individual ions in aqueous single NaCl and $CaCl_2$ electrolyte solutions at the temperature 298.15 K. The model is further tested in this paper for eight 1:1 electrolytes (LiCl, LiBr, NaF, NaCl, NaBr, KF, KCl, and KBr), six 2:1 electrolytes ($MgCl_2$, $MgBr_2$, $CaCl_2$, $CaBr_2$, $BaCl_2$, and $BaBr_2$), one mixed electrolyte (NaCl + $MgCl_2$), one 1:1 electrolyte (NaCl) at various temperatures from 298.15 to 573.15 K, and one 2:1 electrolyte ($MgCl_2$) at various temperatures from 298.15 to 523.15 K, for which the experimental data were compiled by Valiskó and Boda in Ref. 25 and Rowland *et al.* in Ref. 13 from various experimental sources in Refs. 26–35.

a)Author to whom correspondence should be addressed: jlliu@mx.nthu.edu.tw
b)E-mail: beisenbe@rush.edu

The PF model is developed to calculate individual ion activities for which experimental measurements and determination,[10,36,37] interpretation of measurement data,[26,37–39] and comparison of different experimental methods[37,40] have been extensively investigated by Wilczek-Vera, Rodil, and Vera in the past two decades. PF results on mean activity coefficients can be compared with experimental measurements using the Debye-Hückel equation of individual ion activities.[5]

In contrast to the Pitzer model, we show that all experimental data sets of individual or mean activity coefficients as a function of variable concentration in single electrolytes or mixtures at various temperatures can be well fitted by the PF model with only 3 parameters at most for each activity-concentration data curve. The model is characterized by three different domains, namely, the Born ion, hydration shell, and remaining solvent domains in which the Born ion domain is most crucial because all activities around an ion are mainly governed by the singular charge of the ion located at the center of the domain. The Born ion domain is defined by the Born radius of the solvated ion, which is unknown and changes with salt concentrations in a highly nonlinear manner.

The three parameters characterize three orders of approximation of the Born radius in terms of ionic concentrations. Parameter 1 describes a correction of the experimental Born radius of a single ion in pure water without any other ions. Parameter 2 describes an adjustment of the unknown Born radius in electrolyte solution that accounts for the Debye screening effect, which is proportional to the square root of the ionic strength of the solution. Parameter 3 is an adjustment in the next order approximation beyond the DH treatment of ionic atmosphere. The physical origin of these parameters is clear unlike that of most parameters in the Pitzer method.[11,41] It may even be possible in later work to calculate some of these parameters from more detailed versions of our model.

Our approach to partition the free energy domain of a solvated ion into the above three sub-domains yields a better approximation to calculate the free energy since these sub-domains are determined by the experimental data of solvation and thus separate short- and long-range interactions of the ion in a more accurate way. This approach nevertheless incurs more complicated numerical methods for solving the nonlinear partial differential equations of the PF model in different domains with suitable interface conditions.[17] We therefore present numerical methods in detail for future verification and development of the present work.

II. THEORY

For an aqueous electrolyte solution with K species of ions, the Poisson-Fermi theory proposed in Refs. 18 and 21 treats all ions and water of any diameter as nonuniform hard spheres with interstitial voids between these spheres. The activity coefficient γ_i of an ion of species i in the solution describes the deviation of the chemical potential of the ion from ideality ($\gamma_i = 1$). The excess chemical potential $\mu_i^{\text{ex}} = k_B T \ln \gamma_i$ can be calculated by[19,42]

$$\mu_i^{\text{ex}} = \Delta G_i - \Delta G_i^0,\ \Delta G_i = \frac{1}{2} q_i \phi(\mathbf{0}),\ \Delta G_i^0 = \frac{1}{2} q_i \phi^0(\mathbf{0}), \quad (1)$$

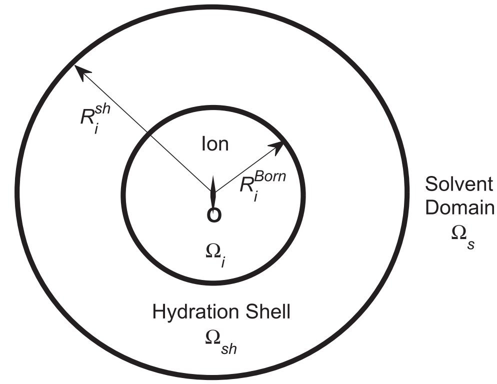

FIG. 1. The model domain Ω is partitioned into the ion domain Ω_i (with radius R_i^{Born}), the hydration shell domain Ω_{sh} (with radius R_i^{sh}), and the remaining solvent domain Ω_s.

where k_B is the Boltzmann constant, T is an absolute temperature, q_i is the ionic charge of the hydrated ion (also denoted by i), $\phi(\mathbf{r})$ is a potential function of spatial variable $\mathbf{r}$ in the domain $\Omega = \overline{\Omega}_i \cup \overline{\Omega}_{sh} \cup \Omega_s$ shown in Fig. 1, Ω_i is the spherical domain occupied by the ion i, Ω_{sh} is the hydration shell domain of the ion, Ω_s is the remaining solvent domain, $\mathbf{0}$ denotes the center (set to the origin) of the ion, $\phi(\mathbf{0})$ is the value of $\phi(\mathbf{r})$ at $\mathbf{r} = \mathbf{0}$, and $\phi^0(\mathbf{r})$ is a potential function when the solvent domain Ω_s does not contain any ion at all with pure water only. The potential function $\phi(\mathbf{r})$ can be found by solving the Poisson-Fermi equation[18]

$$\left(l_c^2 \nabla^2 - 1\right) \nabla \cdot \epsilon(\mathbf{r}) \nabla \phi(\mathbf{r}) = \rho(\mathbf{r}), \quad (2)$$

$$\epsilon(\mathbf{r}) = \begin{cases} \epsilon_s = \epsilon_{\text{w}} \epsilon_0 \text{ in } \overline{\Omega}_{sh} \cup \Omega_s \\ \epsilon_i = \epsilon_{\text{ion}} \epsilon_0 \text{ in } \overline{\Omega}_i \end{cases}, l_c = \begin{cases} 2a_j \text{ in } \overline{\Omega}_{sh} \cup \Omega_s \\ 0 \text{ in } \overline{\Omega}_i \end{cases}, \quad (3)$$

$$\rho(\mathbf{r}) = \begin{cases} \rho_s(\mathbf{r}) = \sum_{k=1}^{K} q_k C_k(\mathbf{r}) \text{ in } \Omega_s \\ 0 \text{ in } \overline{\Omega}_{sh} \\ \rho_i(\mathbf{r}) = q_i \delta(\mathbf{r} - \mathbf{0}) \text{ in } \overline{\Omega}_i \end{cases}, \quad (4)$$

$$C_k(\mathbf{r}) = C_k^{\text{B}} \exp\left(-\beta_k \phi(\mathbf{r}) + \frac{v_k}{v_0} S^{\text{trc}}(\mathbf{r})\right) \text{ in } \overline{\Omega}, \quad (5)$$

$$S^{\text{trc}}(\mathbf{r}) = \ln\left(\frac{\Gamma(\mathbf{r})}{\Gamma^{\text{B}}}\right) \text{ in } \overline{\Omega}, \quad (6)$$

where ϵ_0 is the vacuum permittivity, ϵ_{w} is the dielectric constant of bulk water, ϵ_{ion} is a dielectric constant in $\overline{\Omega}_i$, a_j is the radius of a counterion of the ion i, and $\delta(\mathbf{r} - \mathbf{0})$ is the delta function at the origin.

The concentration function $C_k(\mathbf{r})$ is described by a Fermi distribution (5), where C_k^{B} is a constant bulk concentration for all $k = 1, \ldots, K+1$, $q_{K+1} = 0$, $\beta_k = q_k / k_B T$, $v_k = 4\pi a_k^3/3$, $v_0 = \left(\sum_{k=1}^{K+1} v_k\right)/(K+1)$ an average volume of all kinds of hard spheres, $S^{\text{trc}}(\mathbf{r})$ is called the steric potential, $\Gamma^{\text{B}} = 1 - \sum_{k=1}^{K+1} v_k C_k^{\text{B}}$ is a constant void fraction, $\Gamma(\mathbf{r}) = 1 - \sum_{k=1}^{K+1} v_k C_k(\mathbf{r})$ is a void fraction function, and $K+1$ denotes water. The radii of Ω_i and the outer boundary of Ω_{sh} are denoted by R_i^{Born} and R_i^{sh}, respectively, whose values will be determined by experimental data. It is natural to choose the Born radius R_i^{Born} (not the ionic radius a_i) as the radius of Ω_i.[42] We consider both first and second shells of the ion.[43,44]

The potential $\phi^0(\mathbf{r})$ [in Eq. (1)] of the ideal system is obtained by setting $\rho_s(\mathbf{r}) = 0$ in (4), i.e., all particles in Ω_s do not electrostatically interact with each other since $q_k = 0$ for all k. The domain Ω is chosen to be sufficiently large so that $\phi(\mathbf{r}) = 0$ on the boundary of the domain $\partial\Omega$. The ideal potential $\phi^0(\mathbf{r})$ is then a constant, i.e., ΔG_i^0 is a constant reference chemical potential independent of C_k^{B}.

The distribution (5) is of Fermi type since all concentration functions have an upper bound, i.e., $C_k(\mathbf{r}) < 1/v_k$ for all particle species with any arbitrary (or even infinite) potential $\phi(\mathbf{r})$ at any location $\mathbf{r}$ in the domain Ω.[21] The Poisson-Fermi equation (2) and the Fermi distribution (5) reduce to the Poisson-Boltzmann equation and the Boltzmann distribution when $l_c = S^{\mathrm{trc}} = 0$, i.e., when the correlation and steric effects are not considered. The Boltzmann distribution $C_k(\mathbf{r}) = C_k^{\mathrm{B}} \exp(-\beta_k \phi(\mathbf{r}))$ would however diverge if $\phi(\mathbf{r})$ tends to infinity. This is a major deficiency of the PB theory for modeling a system with strong local electric fields or interactions.[45] If the correlation length $l_c \neq 0$, the dielectric operator $\widehat{\epsilon} = \epsilon_s(1 - l_c^2\nabla^2)$ in Eq. (2) approximates the permittivity of the bulk solvent and the linear response of correlated ions[17,20,46,47] and yields a dielectric function $\widetilde{\epsilon}(\mathbf{r})$ as an output of solving Eq. (2).[21] The exact value of $\widetilde{\epsilon}(\mathbf{r})$ at any $\mathbf{r} \in \overline{\Omega}_{sh} \cup \Omega_s$ cannot be obtained from Eq. (2) but can be approximated by the simple formula $\widetilde{\epsilon}(\mathbf{r}) \approx \epsilon_i + C_{\mathrm{H_2O}}(\mathbf{r})(\epsilon_s - \epsilon_i)/C_{\mathrm{H_2O}}^{\mathrm{B}}$ since the water density function $C_{\mathrm{H_2O}}(\mathbf{r}) = C_{K+1}(\mathbf{r})$ is an output of Eq. (5). This formula is only for visualizing (approximately) the profile of $\widehat{\epsilon}$ or $\widetilde{\epsilon}$. It is not an input of calculation. The input is the correlation length l_c in Eq. (3).[17,20,46,47] The actual outputs are the numerical solutions of the partial differential equations and boundary conditions.

The factor v_k/v_0 multiplying the steric potential function $S^{\mathrm{trc}}(\mathbf{r})$ in Eq. (5) is a modification of the unity used in our previous work.[19,21] The steric energy $-\frac{v_k}{v_0} S^{\mathrm{trc}}(\mathbf{r}) k_B T$[21,24] of a type k particle depends not only on the voidness ($\Gamma(\mathbf{r})$) (or equivalently crowding) at $\mathbf{r}$ but also on the volume v_k of the particle itself. If all v_k are equal (and thus $v_k = v_0$), then all particle species at any location $\mathbf{r} \in \overline{\Omega}_{sh} \cup \Omega_s$ have the same steric energy, i.e., uniform particles are indistinguishable in steric energy. The steric potential is a mean-field approximation of Lennard-Jones (L-J) potentials that describe local variations of L-J distances (and thus empty voids) between any pair of particles. L-J potentials are highly oscillatory and extremely expensive and unstable to compute numerically.[21] Calculations that involve L-J potentials or even truncated versions of L-J potentials must be extensively checked to be sure that results do not depend on irrelevant parameters.

III. METHODS

To avoid large errors in approximation caused by the delta function $\delta(\mathbf{r} - \mathbf{0})$ in (4), the potential function can be decomposed as[17,48,49]

$$\phi(\mathbf{r}) = \begin{cases} \widetilde{\phi}(\mathbf{r}) + \phi^*(\mathbf{r}) + \phi^{\mathrm{L}}(\mathbf{r}) \text{ in } \Omega_i \\ \widetilde{\phi}(\mathbf{r}) \text{ in } \overline{\Omega}_{sh} \cup \Omega_s \end{cases}, \tag{7}$$

where $\phi^*(\mathbf{r}) = q_i/(4\pi\epsilon_i |\mathbf{r} - \mathbf{0}|)$ and $\widetilde{\phi}(\mathbf{r})$ is found by solving

$$\left(l_c^2\nabla^2 - 1\right) \nabla \cdot \epsilon_s \nabla \widetilde{\phi}(\mathbf{r}) = \rho(\mathbf{r}) \text{ in } \overline{\Omega}_{sh} \cup \Omega_s, \tag{8}$$

$$-\nabla \cdot \epsilon_i \nabla \widetilde{\phi}(\mathbf{r}) = 0 \ \text{ in } \Omega_i \tag{9}$$

without the singular source term $\rho_i(\mathbf{r}) = q_i \delta(\mathbf{r} - \mathbf{0})$ and with the interface conditions

$$\begin{cases} \left[\widetilde{\phi}(\mathbf{r})\right] = 0 \\ \left[\epsilon(\mathbf{r})\nabla\widetilde{\phi}(\mathbf{r}) \cdot \mathbf{n}\right] = \epsilon_i \nabla \left(\phi^*(\mathbf{r}) + \phi^{\mathrm{L}}(\mathbf{r})\right) \cdot \mathbf{n} \end{cases} \text{for all } \mathbf{r} \in \partial\Omega_i, \tag{10}$$

where $\mathbf{n}$ is an outward normal unit vector at $\mathbf{r} \in \partial\Omega_i$ and the jump function $[u(\mathbf{r})] = \lim_{\mathbf{r}_{sh} \to \mathbf{r}} u(\mathbf{r}_{sh}) - \lim_{\mathbf{r}_i \to \mathbf{r}} u(\mathbf{r}_i)$ with $\mathbf{r}_{sh} \in \Omega_{sh}$ and $\mathbf{r}_i \in \Omega_i$.[17] The potential function $\phi^{\mathrm{L}}(\mathbf{r})$ is the solution of the Laplace equation

$$\nabla^2 \phi^{\mathrm{L}}(\mathbf{r}) = 0 \text{ in } \Omega_i \tag{11}$$

with the boundary condition

$$\phi^{\mathrm{L}}(\mathbf{r}) = \phi^*(\mathbf{r}) \text{ on } \partial\Omega_i. \tag{12}$$

The evaluation of Green's function $\phi^*(\mathbf{r})$ on $\partial\Omega_i$ always yields finite numbers and thus avoids the singularity in the solution process. The desired solvation energy ΔG_i in Eq. (1) (and thus the individual ionic activity coefficient γ_i) is then evaluated by[17,49]

$$\Delta G_i = k_B T \ln \gamma_i = \frac{1}{2} q_i \left[\widetilde{\phi}(\mathbf{0}) + \phi^{\mathrm{L}}(\mathbf{0})\right]. \tag{13}$$

Since the interface $\partial\Omega_i$ is a sphere centered at the origin, the Laplace potential $\phi^{\mathrm{L}}(\mathbf{r}) = q_i/(4\pi\epsilon_i R_i^{Born})$ is a constant in $\overline{\Omega}_i$, i.e., Eq. (11) has been exactly solved.

The Poisson-Fermi equation (8) is a nonlinear fourth-order partial differential equation (PDE) in Ω_s. Newton's iterative method is usually used for solving nonlinear problems. We seek a sequence of approximate solutions $\left\{\widetilde{\phi}_m(\mathbf{r})\right\}_{m=1}^M$ by iteratively solving the linearized PF equation

$$\left(l_c^2\nabla^2 - 1\right) \nabla \cdot \epsilon \nabla \widetilde{\phi}_m - \rho_s'(\widetilde{\phi}_{m-1})\widetilde{\phi}_m = \rho_s(\widetilde{\phi}_{m-1}) - \rho_s'(\widetilde{\phi}_{m-1})\widetilde{\phi}_{m-1} \text{ in } \Omega_s, \tag{14}$$

until a tolerable potential function $\widetilde{\phi}_M$ is reached, where $\widetilde{\phi}_0(\mathbf{r})$ is a given initial guess potential function, $\rho_s(\widetilde{\phi}_{m-1}) = \sum_{k=1}^K q_k C_k^{m-1}(\mathbf{r})$, $C_k^{m-1}(\mathbf{r}) = C_k^{\mathrm{B}} \exp\left(-\beta_k \widetilde{\phi}_{m-1}(\mathbf{r}) + \frac{v_k}{v_0} S_{m-1}^{\mathrm{trc}}(\mathbf{r})\right)$, $S_{m-1}^{\mathrm{trc}}(\mathbf{r}) = \ln\left(\frac{\Gamma_0(\mathbf{r})}{\Gamma^{\mathrm{B}}}\right)$, $\Gamma_{m-1}(\mathbf{r}) = 1 - \sum_{k=1}^{K+1} v_k C_k^{m-1}(\mathbf{r})$, $\rho_s'(\widetilde{\phi}_{m-1}) = \sum_{k=1}^K (-\beta_k q_k) C_k^{m-1}(\mathbf{r})$, and $\rho_s'(\widetilde{\phi}) = \frac{d}{d\widetilde{\phi}} \rho_s(\widetilde{\phi})$. Note that the differentiation in $\rho_s'(\widetilde{\phi})$ is performed only with respect to $\widetilde{\phi}$, whereas S^{trc} is treated as another independent variable although S^{trc} depends on $\widetilde{\phi}$ as well. Therefore, $\rho_s'(\widetilde{\phi})$ is not exact implying that this is an inexact Newton's method.[50]

The fourth-order problem can be resolved by transforming Eq. (14) into two second-order PDEs[17]

$$\epsilon_s \left(l_c^2\nabla^2 - 1\right) \Psi(\mathbf{r}) = \rho(\widetilde{\phi}_{m-1}) \text{ in } \overline{\Omega}_{sh} \cup \Omega_s, \tag{15}$$

$$-\epsilon_s \nabla^2 \widetilde{\phi}_m(\mathbf{r}) - \rho'(\widetilde{\phi}_{m-1})\widetilde{\phi}_m(\mathbf{r}) = -\epsilon_s \Psi(\mathbf{r}) - \rho'(\widetilde{\phi}_{m-1})\widetilde{\phi}_{m-1} \text{ in } \overline{\Omega}_{sh} \cup \Omega_s \tag{16}$$

by introducing a density like variable $\Psi = \nabla^2 \widetilde{\phi}$ for which the boundary condition is[17]

$$\Psi(\mathbf{r}) = 0 \text{ on } \partial\Omega_s. \tag{17}$$

Equations (9), (15), and (16) are coupled together in the entire domain Ω with the jump conditions in (10). Note that linear PDEs (14)–(16) converge to the nonlinear PDE (8) if $\widetilde{\phi}_M$ converges to the exact solution $\widetilde{\phi}$ of Eq. (8) as $M \to \infty$, i.e., the approximate potential $\widetilde{\phi}_M(\mathbf{r})$ is sufficiently close to the exact potential $\widetilde{\phi}(\mathbf{r})$ for all $\mathbf{r} \in \overline{\Omega}_{sh} \cup \Omega_s$ if the iteration number M is sufficiently large ($M \approx$ 5–37 for this work with error tolerance 10^{-3}).

The standard 7-point finite difference (FD) method is used to discretize all PDEs (9), (15), and (16), where the jump conditions in (10) are handled by the simplified matched interface and boundary (SMIB) method proposed in Ref. 17. For simplicity, the SMIB method is illustrated by the following 1D linear Poisson equation (in x-axis):

$$-\frac{d}{dx}\left[\epsilon(x)\frac{d}{dx}\widetilde{\phi}(x)\right] = f(x) \text{ in } \Omega \tag{18}$$

with the jump condition

$$\left[\epsilon\widetilde{\phi}'\right] = -\epsilon_i \frac{d}{dx}\phi^*(x) \text{ at } x = \xi = \partial\Omega_i \cap \partial\Omega_s, \tag{19}$$

where $\Omega = \Omega_i \cup \Omega_s$, $\Omega_i = (0, \xi)$, $\Omega_s = (\xi, L)$, $f(x) = 0$ in Ω_i, $f(x) \neq 0$ in Ω_s, and $\widetilde{\phi}' = \frac{d}{dx}\widetilde{\phi}(x)$. The corresponding cases to Eqs. (9), (15), and (16) in the y- and z-axis follow in a similar way. Let two FD grid points x_l and x_{l+1} across the interface point ξ be such that $x_l < \xi < x_{l+1}$ and $\xi = (x_l + x_{l+1})/2$ with $\Delta x = x_{l+1} - x_l = 1$ Å, a uniform mesh, for example, as used in this work. The FD equations of the SMIB method at x_l and x_{l+1} are

$$\epsilon_i \frac{-\widetilde{\phi}_{l-1} + (2 - c_1)\widetilde{\phi}_l - c_2\widetilde{\phi}_{l+1}}{\Delta x^2} = f_l + \frac{c_0}{\Delta x^2}, \tag{20}$$

$$\epsilon_s \frac{-d_1\widetilde{\phi}_l + (2 - d_2)\widetilde{\phi}_{l+1} - \widetilde{\phi}_{l+2}}{\Delta x^2} = f_{l+1} + \frac{d_0}{\Delta x^2}, \tag{21}$$

where

$$c_1 = \frac{\epsilon_i - \epsilon_s}{\epsilon_i + \epsilon_s}, c_2 = \frac{2\epsilon_s}{\epsilon_i + \epsilon_s}, c_0 = \frac{-\epsilon_i\Delta x\left[\epsilon\widetilde{\phi}'\right]}{\epsilon_i + \epsilon_s},$$
$$d_1 = \frac{2\epsilon_i}{\epsilon_i + \epsilon_s}, d_2 = \frac{\epsilon_s - \epsilon_i}{\epsilon_i + \epsilon_s}, d_0 = \frac{-\epsilon_s\Delta x\left[\epsilon\widetilde{\phi}'\right]}{\epsilon_i + \epsilon_s},$$

$\widetilde{\phi}_l$ is an approximation of $\widetilde{\phi}(x_l)$, and $f_l = f(x_l)$. Note that the jump value $\left[\epsilon\widetilde{\phi}'\right]$ at ξ is calculated exactly since the derivative of ϕ^* is given analytically.

Since the steric potential takes particle volumes and voids into account, the shell volume V_{sh} of the shell domain Ω_{sh} can be determined by Eqs. (5) and (6) as

$$S_{sh}^{\text{trc}} = \frac{v_0}{v_{\text{w}}}\ln\left(\frac{O_i^{\text{w}}}{V_{sh}C_{K+1}^{\text{B}}}\right) = \ln\left(\frac{V_{sh} - v_{\text{w}}O_i^{\text{w}}}{V_{sh}\Gamma^{\text{B}}}\right), \tag{22}$$

where the occupancy (coordination) number O_i^{w} is given by experimental data.[43,44] The shell radius R_i^{sh} of Ω_{sh} is thus determined. Note that the shell volume depends not only on O_i^{w} but also on the bulk void fraction Γ^{B}, namely, **on all salt and water concentrations** (C_k^{B}).

As discussed in Ref. 25, the solvation free energy of an ion i should vary with salt concentrations and can be expressed by a dielectric constant $\epsilon(C_i^{\text{B}})$ that depends on the bulk concentration C_i^{B} of the ion. Therefore, the Born energy

$$\Delta G_i^{\text{Born}} = \left(\frac{1}{\epsilon_{\text{w}}} - 1\right)\frac{q_i^2}{8\pi\epsilon_0 R_i^0} \tag{23}$$

with the Born radius R_i^0 in pure water should be modified with the concentration-dependent dielectric constant $\epsilon(C_i^{\text{B}})$. Equivalently, the Born radius in electrolyte solutions can be modified from R_i^0 by a simple formula

$$R_i^{Born}(C_i^{\text{B}}) = \theta(C_i^{\text{B}})R_i^0,$$
$$\theta(C_i^{\text{B}}) = \alpha_1^i + \alpha_2^i\left(\overline{C}_i^{\text{B}}\right)^{1/2} + \alpha_3^i\left(\overline{C}_i^{\text{B}}\right)^{3/2}, \tag{24}$$

where $\overline{C}_i^{\text{B}} = C_i^{\text{B}}/\text{M}$ is a dimensionless bulk concentration of type i ions, M is the molar concentration unit, and α_1^i, α_2^i, and α_3^i are adjustable parameters for modifying the experimental Born radius R_i^0 to fit experimental activity coefficients γ_i that change with the bulk concentration conditions C_i^{B} of the ion. The Born radii R_i^0 in Table I are cited from Ref. 25, which are computed from the experimental hydration Helmholtz free energies of these ions given in Ref. 6. Numerical values in Tables I and II are all experimental data for which their values are kept fixed throughout calculations once chosen.

The three parameters in Eq. (24) have physical or mathematical meaning unlike many parameters in the Pitzer model.[41] Any model or numerical method incurs errors to approximate a real system, i.e., it is impossible to obtain real Born radius $R_i^{Born}(C_i^{\text{B}})$ exactly. The first parameter α_1^i is an adjustment of the experimental Born radius R_i^0 when $C_i^{\text{B}} = 0$ for all i. The second parameter α_2^i is an adjustment of $R_i^{Born}(C_i^{\text{B}})$ that accounts for the real thickness of the ionic atmosphere (Debye length), which is proportional to the square root of the ionic strength $\sqrt{I}$ in the Debye-Hückel theory.[5] The third parameter α_3^i is simply an adjustment in the

TABLE I. Values of model notations.

Symbol	Meaning	Value	Unit
k_B	Boltzmann constant	1.38×10^{-23}	J/K
T	Temperature	Table II	K
e	Proton charge	1.602×10^{-19}	C
ϵ_0	Permittivity of vacuum	8.85×10^{-14}	F/cm
$\epsilon_{\text{ion}}, \epsilon_{\text{w}}$	Dielectric constants	1, Table II	
$l_c = 2a_j$	Correlation length	$j = \text{Cl}^-$, etc.	Å
O_i^{w}	In Eq. (22)	18[43,44]	
$a_{\text{Li}^+}, a_{\text{Na}^+}, a_{\text{K}^+}$	Radii	0.6, 0.95, 1.33	Å
$a_{\text{Mg}^{2+}}, a_{\text{Ca}^{2+}}, a_{\text{Ba}^{2+}}$	Radii	0.65, 0.99, 1.35	Å
$a_{\text{F}^-}, a_{\text{Cl}^-}, a_{\text{Br}^-}, a_{\text{H}_2\text{O}}$	Radii	1.36, 1.81, 1.95, 1.4	Å
$R^0_{\text{Li}^+}, R^0_{\text{Na}^+}, R^0_{\text{K}^+}$	Born radii in Eq. (24)	1.3, 1.618, 1.95	Å
$R^0_{\text{Mg}^{2+}}, R^0_{\text{Ca}^{2+}}, R^0_{\text{Ba}^{2+}}$	Born radii	1.424, 1.708, 2.03	Å
$R^0_{\text{F}^-}, R^0_{\text{Cl}^-}, R^0_{\text{Br}^-},$	Born radii	1.6, 2.266, 2.47	Å

TABLE II. Values of ϵ_{w} at various T.[51]

T/K	298.15	373.15	423.15	473.15	523.15	573.15
ϵ_{w}	78.41	55.51	44.04	38.23	32.23	25.07

next order approximation beyond the DH treatment of ionic atmosphere.

We summarize the mathematical solution process for determining the activity of ionic solutions in the following algorithm.

1. Solve Eqs. (9), (10), and (16) for $\widetilde{\phi}$ with $\rho' = \Psi = 0$ (in pure water), $R_i^{Born} = R_i^0$, and $\phi^{\mathrm{L}} = q_i/(4\pi\epsilon_i R_i^0)$ to obtain ΔG_i^0 by Eq. (13) and then set $\widetilde{\phi}_0 = \widetilde{\phi}$.
2. Solve Eqs. (15) and (17) for Ψ with R_i^{Born} in (24).
3. Solve Eqs. (9), (10), and (16) for $\widetilde{\phi}_m$ with $\phi^{\mathrm{L}} = q_i/(4\pi\epsilon_i R_i^{Born})$ and then set $\widetilde{\phi}_{m-1} = \widetilde{\phi}_m$. Go to 2 until convergence.
4. Obtain the activity coefficient γ_i by Eq. (13).

IV. RESULTS

The PF results of ionic activity coefficients for eight 1:1 electrolytes, six 2:1 electrolytes, one mixed electrolyte, one 1:1 electrolyte at various temperatures, and one 2:1 electrolyte at various temperatures agree with the experimental data[26–35] as shown in Figs. 2–6, respectively. The empirical parameters used to fit the experimental data are α_1^i, α_2^i, and α_3^i in Eq. (24), whose values are given in Table III from which we observe that the PF model requires only one to three parameters to fit those data.

The mean activity coefficient γ_{PosNeg} of a salt $\mathrm{Pos}_p\mathrm{Neg}_q$ is calculated via the formula $\ln\gamma_{PosNeg} = \frac{p}{p+q}\ln\gamma_{Pos} + \frac{q}{p+q}\ln\gamma_{Neg}$,[5] where γ_{Pos} and γ_{Neg} are individual activity coefficients obtained by Eq. (13) for each $i = Pos$ and Neg. For the mean activity coefficients of either ternary (Fig. 4) or binary (Figs. 5 and 6) systems, we only need to adjust 3 parameters of one cation (not all ions) as shown in Table III.

The activity coefficients by the PF model are quite successful over a large range of temperatures and concentrations as shown in Figs. 4–6. We used the code of the density model developed by Mao and Duan[52] to convert the concentration unit from molality (mol Kg^{-1}) to molarity ($\mathrm{M} = \mathrm{mol\ dm}^{-3}$) by the standard formula as given in Ref. 52, where the density model has been compared with thousands of measurements at high accuracy. The pressure values needed in the code at the corresponding temperatures were set to P = (a) 1.01, (b) 1.01, (c) 15.48, (d) 39.59, and (e) 80.50 bars for Fig. 5 and (a) 1.01, (b) 1.01, (c) 4.73, and (d) 39.50 bars for Fig. 6. In Fig. 4, the ionic strength $I = \sum_i C_i^{\mathrm{B}} z_i^2$ and the ionic strength fraction $y_{\mathrm{MgCl}_2} = 3m_{\mathrm{MgCl}_2}/(3m_{\mathrm{MgCl}_2} + m_{\mathrm{NaCl}})$ with m_{MgCl_2} and m_{NaCl} being the molalities of MgCl_2 and NaCl

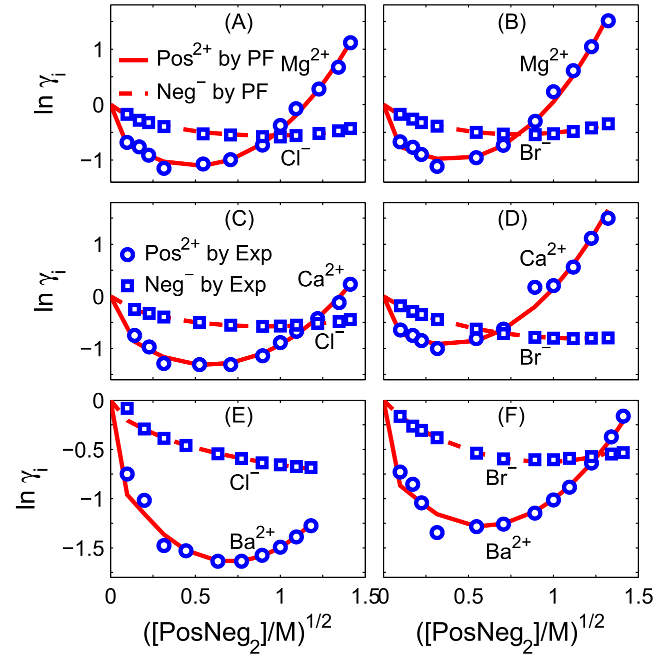

FIG. 3. Individual activity coefficients of 2:1 electrolytes. Comparison of PF results with experimental data[26] on $i = \mathrm{Pos}^{2+}$ (cation) and Neg^- (anion) activity coefficients γ_i in various $[\mathrm{PosNeg}_2]$ from 0 to 1.5M.

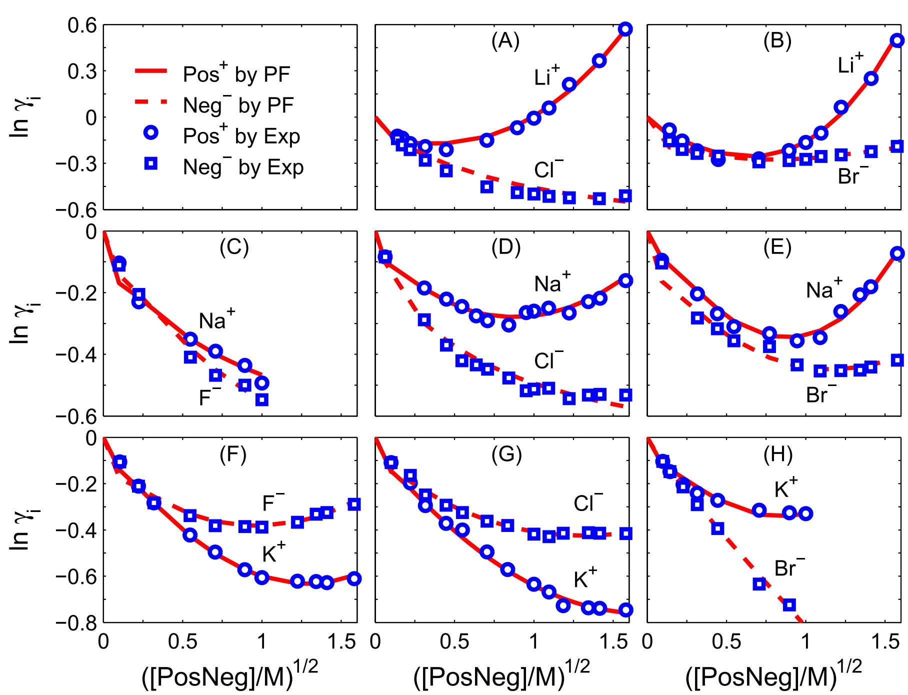

FIG. 2. Individual activity coefficients of 1:1 electrolytes. Comparison of PF results with experimental data[26] on $i = \mathrm{Pos}^+$ (cation) and Neg^- (anion) activity coefficients γ_i in various [PosNeg] from 0 to 1.6M.

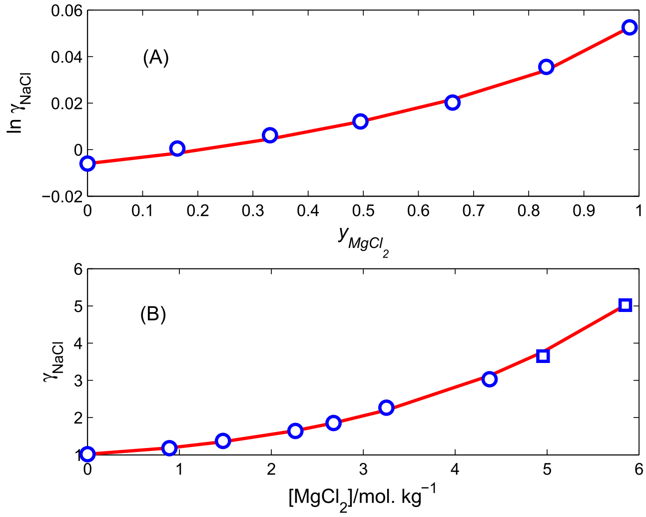

FIG. 4. Mean activity coefficients of mixed electrolytes. Comparison of PF results (curve) with experimental data (symbols) compiled in Ref. 13 (a) from Ref. 33 on mean activity coefficients γ of NaCl as a function of the ionic strength (I) fraction $y_{\mathrm{MgCl_2}}$ of $MgCl_2$ in NaCl + $MgCl_2$ mixtures at I = 6 mol Kg^{-1} and T = 298.15 K and (b) from Ref. 34 (circles) and Ref. 35 (squares) on γ of NaCl as a function of the $MgCl_2$ molality in NaCl + $MgCl_2$ mixtures at [NaCl] = 6 mol Kg^{-1} and T = 298.15 K.

in the mixture, respectively, where z_i is the valence of type i ions.

We observe from Table III that the approximate $R_i^{Born}(C_i^{\mathrm{B}})$ (with salts) deviates from R_i^0 (without salts) only in the second to fourth decimal place, i.e., numerical values of γ_i are very sensitive to the decimal order of α_1^i, α_2^i, and α_3^i because the Born radius $R_i^{Born}(C_i^{\mathrm{B}})$ is very close to the origin $\mathbf{0}$ at which the singular charge in $\rho_i(\mathbf{r}) = q_i\delta(\mathbf{r}-\mathbf{0})$ is infinite. The approximation of the shell radius R_i^{Sh} [or the coordination number O_i^{w} in Eq. (22)], on the other hand, is much less significant than that of R_i^{Born} because the electric potential $\phi^{\mathrm{PF}}(\mathbf{r})$ diminishes exponentially in the hydration shell region Ω_{sh} as shown by

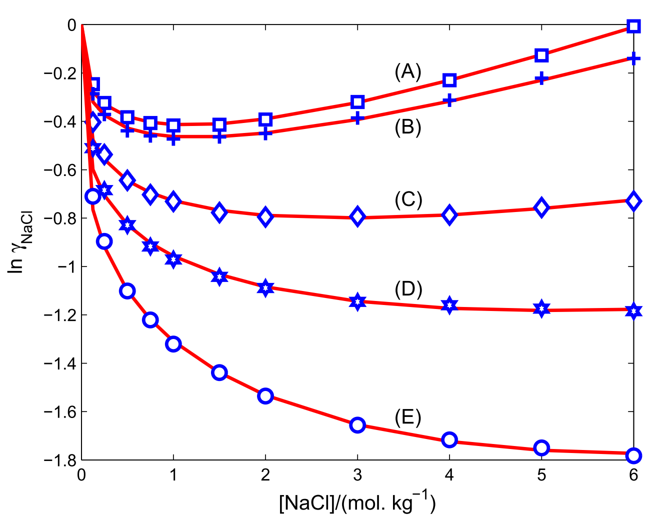

FIG. 5. Mean activity coefficients of 1:1 electrolyte at various temperatures. Comparison of PF results (curves) with experimental data (symbols) compiled in Ref. 13 from Refs. 27–29 on mean activity coefficients γ of NaCl in [NaCl] from 0 to 6 mol Kg^{-1} at T = (a) 298.15, (b) 373.15, (c) 473.15, (d) 523.15, (e) 573.15 K.

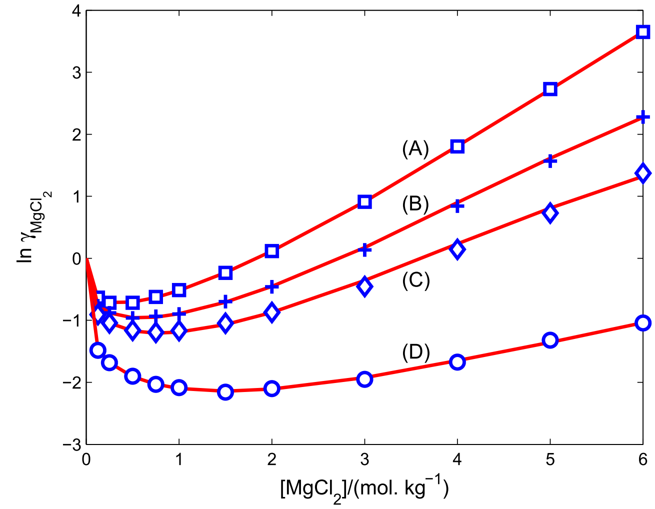

FIG. 6. Mean activity coefficients of 2:1 electrolyte at various temperatures. Comparison of PF results (curves) with experimental data (symbols) compiled in Ref. 13 from Refs. 30–32 on mean activity coefficients γ of $MgCl_2$ in [$MgCl_2$] from 0 to 6 mol Kg^{-1} at T = (a) 298.15, (b) 373.15, (c) 423.15, (d) 523.15 K.

the profile of $\phi^{\mathrm{PF}}(\mathbf{r})$ in Fig. 7. The values of α_1^i, α_2^i, and α_3^i for each activity-concentration curve were obtained by first tuning three values of $\theta(C_i^{\mathrm{B}})$ in Eq. (24) to match three data points $(\sqrt{C_{ij}^{\mathrm{B}}}, \ln\gamma_{ij})$ with three different concentrations C_{ij}^{B}, j = 1, 2, 3, and then solving the three unknowns α_1^i, α_2^i, and α_3^i using three known $\theta(C_{ij}^{\mathrm{B}})$ values. For example, for the $i = \mathrm{Li}^+$ curve in Fig. 2(a), the selected experimental data points are $(\sqrt{C_{ij}^{\mathrm{B}}}, \ln\gamma_{ij})$ = (0.315, −0.192), (1, −0.007), and (1.577, 0.57) and the corresponding tuned $\theta(C_{ij}^{\mathrm{B}})$ are 0.9996, 1.0013, and 1.0043.

The PF model can provide more physical details near the solvated ion (Ca^{2+}, for example) in a strong electrolyte ([$CaCl_2$] = 2M) such as (1) the dielectric function $\widetilde{\epsilon}(\mathbf{r})$ with its varying permittivity, (2) variable water density $C_{\mathrm{H_2O}}(\mathbf{r})$, (3) concentration of counterion $C_{\mathrm{Cl^-}}(\mathbf{r})$, (4) electric potential $\phi^{\mathrm{PF}}(\mathbf{r})$, and (5) the steric potential $S^{\mathrm{trc}}(\mathbf{r})$ all shown in Fig. 7. The steric potential is small because the configuration of particles (voids between particles) does not vary too much from the solvated region to the bulk region. Nevertheless, it has significant effect on the variation of mean-field water densities $C_{\mathrm{H_2O}}(\mathbf{r})$ and hence on the dielectric function $\widetilde{\epsilon}(\mathbf{r})$ in the hydration region. Note that $\widetilde{\epsilon}(\mathbf{r})$ is an output, not an input of the model.

The strong electric potential $\phi^{\mathrm{PF}}(\mathbf{r})$ in the Born cavity $\overline{\Omega}_i$ (with $R_i^{Born}(C_i^{\mathrm{B}})$ = 1.7130 Å) and the water density $C_{\mathrm{H_2O}}(\mathbf{r})$ in the hydration shell Ω_{sh} (with $R_{\mathrm{Ca^{2+}}}^{sh}$ = 5.0769 Å) are the most important factors allowing the PF results to match the experimental data. The ion and shell domains are the crucial region to study ion activities. For example, Fraenkel's theory is entirely based on this region—the so-called smaller-ion shell region.[41] The steric energy of water molecules modified by the factor v_{K+1}/v_0 in Eq. (5) leads to significant changes of $C_{\mathrm{H_2O}}(\mathbf{r})$ and $\widetilde{\epsilon}(\mathbf{r})$ profiles in Fig. 7 as compared with those in Fig. 5 in our previous paper.[19]

TABLE III. Values of α_1^i, α_2^i, and α_3^i in Eq. (24).

Figures	i	α_1^i	α_2^i	α_3^i	Figures	i	α_1^i	α_2^i	α_3^i
2(a)	Li^+	0.999 13	0.000 69	0.000 09	3(c)	Ca^{2+}	0.998 86	0.000 46	0.000 11
2(a)	Cl^-	0.998 93	−0.000 08		3(c)	Cl^-	0.998 77	−0.000 60	0.000 12
2(b)	Li^+	0.999 58	−0.000 19	0.000 15	3(d)	Ca^{2+}	0.998 86	0.000 99	0.000 17
2(b)	Br^-	0.998 22	0.001 07		3(d)	Br^-	0.999 20	−0.001 98	0.000 16
2(c)	Na^+	0.999 10			3(e)	Ba^{2+}	0.998 44	0.000 11	0.000 10
2(c)	F^-	0.999 33	−0.000 29		3(e)	Cl^-	0.998 87	−0.000 58	0.000 01
2(d)	Na^+	0.999 27	0.000 26	0.000 04	3(f)	Ba^{2+}	0.998 51	0.000 54	0.000 08
2(d)	Cl^-	0.998 40			3(f)	Br^-	0.999 26	−0.001 45	0.000 18
2(e)	Na^+	0.999 62	−0.000 38	0.000 10	4(a)	Na^+	1.005 81	−0.000 13	
2(e)	Br^-	0.998 70	−0.000 17	0.000 04	4(b)	Na^+	1.005 27	0.000 42	0.000 19
2(f)	K^+	0.999 34	−0.001 20	0.000 07	5(a)	Na^+	0.998 1		0.000 1
2(f)	F^-	0.999 04	0.000 13	0.000 04	5(b)	Na^+	0.997 1	0.000 3	0.000 1
2(g)	K^+	0.999 29	−0.001 22	0.000 04	5(c)	Na^+	0.994 5	−0.000 7	0.000 1
2(g)	Cl^-	0.998 97	−0.000 12	0.000 03	5(d)	Na^+	0.992 5	−0.002 8	0.000 1
2(h)	K^+	0.999 31	0.000 13		5(e)	Na^+	0.987 0	−0.004 2	0.001 0
2(h)	Br^-	0.999 45	−0.001 75	−0.000 06	6(a)	Mg^{2+}	0.998 8	0.000 2	0.000 2
3(a)	Mg^{2+}	0.999 18	0.000 44	0.000 11	6(b)	Mg^{2+}	0.998 9	−0.000 4	0.000 3
3(a)	Cl^-	0.998 93	−0.000 51	0.000 10	6(c)	Mg^{2+}	0.998 3	−0.001 4	0.000 5
3(b)	Mg^{2+}	0.999 10	0.00063	0.000 15	6(d)	Mg^{2+}	0.996 1	−0.002 0	0.000 3
3(b)	Br^-	0.998 88	−0.000 65	0.000 18					

Default values: $\alpha_1^i = 1$, $\alpha_2^i = 0$, and $\alpha_3^i = 0$.

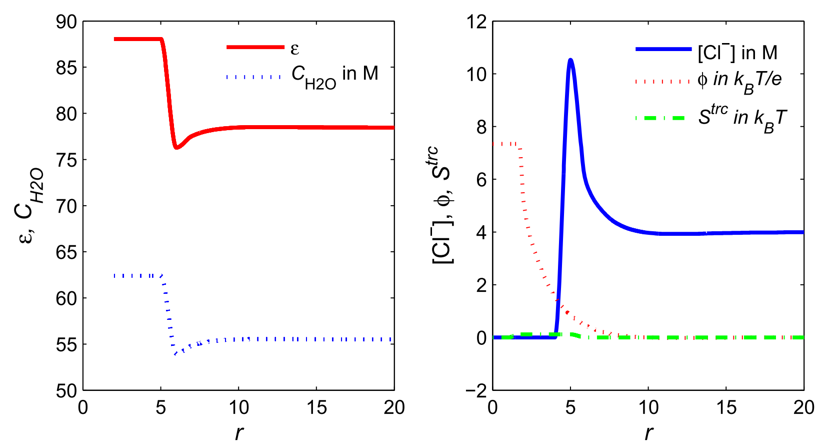

FIG. 7. Dielectric function $\tilde{\epsilon}(\mathbf{r})$ (denoted by ε in the figure), water density $C_{H_2O}(\mathbf{r})$ (C_{H_2O}), Cl^- concentration $C_{Cl^-}(\mathbf{r})$ ([Cl^-]), electric potential $\phi^{PF}(\mathbf{r})$ (ϕ), and steric potential $S^{trc}(\mathbf{r})$ (S^{trc}) profiles near the solvated ion Ca^{2+} at [$CaCl_2$] = 2M, where r is the distance from the center of Ca^{2+} in angstrom.

V. CONCLUSION

A Poisson-Fermi model for calculating activity coefficients of aqueous single or mixed electrolyte solutions in a large range of concentrations and temperatures has been presented and tested by a set of experimental data. The model was shown to well fit experimental data with only three adjustable parameters at most for each activity-concentration curve. The adjustable parameters correspond to different orders of approximation of the unknown Born radius of solvation energy that depends on salt concentrations in a highly complex and nonlinear way. Nevertheless, the values of these parameters have been shown to deviate slightly in decimal digits from that of the experimental Born radius in pure water. These parameters are physically explained and can be easily verified in future studies for the same or different solutions of the present work. The model requires very few parameters because it is based on an advanced continuum theory that accounts for steric and correlation effects of ions and water with interstitial voids between nonuniform hard spheres. It also deals with short- and long-range interactions by partitioning the model domain into the ion, hydration shell, and the remaining solvent sub-domains. Numerical methods were also given to show how to solve different equations on different sub-domains that describe different physical properties of an ion in electrolyte solutions.

ACKNOWLEDGMENTS

This work was supported by the Ministry of Science and Technology, Taiwan (No. MOST 105-2115-M-007-016-MY2 to J.-L.L.).

[1] R. Robinson and R. Stokes, *Electrolyte Solutions* (Butterworths Scientific Publications, London, 1959); (Dover Publications, New York, 2002).
[2] J. Newman, *Electrochemical Systems* (Prentice-Hall, NJ, 1991).
[3] K. S. Pitzer, *Thermodynamics* (McGraw Hill, New York, 1995).
[4] B. Hille, *Ionic Channels of Excitable Membranes* (Sinauer Associates, Inc., Sunderland, MA, 2001).

[5] K. J. Laidler, J. H. Meiser, and B. C. Sanctuary, *Physical Chemistry* (Houghton Mifflin Co., Boston, 2003).

[6] W. R. Fawcett, *Liquids, Solutions, and Interfaces: From Classical Macroscopic Descriptions to Modern Microscopic Details* (Oxford University Press, New York, 2004).

[7] G. Lebon, D. Jou, and J. Casas-Vázquez, *Understanding Non-Equilibrium Thermodynamics: Foundations, Applications, Frontiers* (Springer, 2008).

[8] G. M. Kontogeorgis and G. K. Folas, *Thermodynamic Models for Industrial Applications: From Classical and Advanced Mixing Rules to Association Theories* (John Wiley & Sons, 2009).

[9] W. Kunz, *Specific Ion Effects* (World Scientific, Singapore, 2010).

[10] J. H. Vera and G. Wilczek-Vera, *Classical Thermodynamics of Fluid Systems: Principles and Applications* (CRC Press, 2016).

[11] W. Voigt, "Chemistry of salts in aqueous solutions: Applications, experiments, and theory," Pure Appl. Chem. **83**, 1015–1030 (2011).

[12] B. Eisenberg, "Interacting ions in biophysics: Real is not ideal," Biophys. J. **104**, 1849–1866 (2013).

[13] D. Rowland, E. Königsberger, G. Hefter, and P. M. May, "Aqueous electrolyte solution modelling: Some limitations of the Pitzer equations," Appl. Geochem. **55**, 170 (2015).

[14] P. Debye and E. Hückel, "Zur theorie der elektrolyte. I. Gefrierpunktserniedrigung und verwandte erscheinunge (the theory of electrolytes. I. Lowering of freezing point and related phenomena)," Phys. Z. **24**, 185–206 (1923).

[15] M. Gouy, "Sur la constitution de la charge electrique a la surface d'un electrolyte (constitution of the electric charge at the surface of an electrolyte)," J. Phys. Theor. Appl. **9**, 457–468 (1910).

[16] D. L. Chapman, "A contribution to the theory of electrocapillarity," Philos. Mag. Ser. 6 **25**, 475–481 (1913).

[17] J.-L. Liu, "Numerical methods for the Poisson-Fermi equation in electrolytes," J. Comput. Phys. **247**, 88 (2013).

[18] J.-L. Liu, D. Xie, and B. Eisenberg, "Poisson-Fermi formulation of nonlocal electrostatics in electrolyte solutions," Mol. Based Math. Biol. **5**, 116–124 (2017).

[19] J.-L. Liu and B. Eisenberg, "Poisson-Fermi model of single ion activities in aqueous solutions," Chem. Phys. Lett. **637**, 1–6 (2015).

[20] J.-L. Liu and B. Eisenberg, "Correlated ions in a calcium channel model: A Poisson-Fermi theory," J. Phys. Chem. B **117**, 12051 (2013).

[21] J.-L. Liu and B. Eisenberg, "Poisson-Nernst-Planck-Fermi theory for modeling biological ion channels," J. Chem. Phys. **141**, 22D532 (2014).

[22] J.-L. Liu and B. Eisenberg, "Analytical models of calcium binding in a calcium channel," J. Chem. Phys. **141**, 075102 (2014).

[23] J.-L. Liu and B. Eisenberg, "Numerical methods for a Poisson-Nernst-Planck-Fermi model of biological ion channels," Phys. Rev. E **92**, 012711 (2015).

[24] J.-L. Liu, H.-j. Hsieh, and B. Eisenberg, "Poisson-Fermi modeling of the ion exchange mechanism of the sodium/calcium exchanger," J. Phys. Chem. B **120**, 2658–2669 (2016).

[25] M. Valiskó and D. Boda, "Unraveling the behavior of the individual ionic activity coefficients on the basis of the balance of ion-ion and ion-water interactions," J. Phys. Chem. B **119**, 1546 (2015).

[26] G. Wilczek-Vera, E. Rodil, and J. H. Vera, "On the activity of ions and the junction potential: Revised values for all data," AIChE J. **50**, 445 (2004).

[27] K. S. Pitzer, J. C. Peiper, and R. H. Busey, "Thermodynamic properties of aqueous sodium chloride solutions," J. Phys. Chem. Ref. Data **13**, 1–102 (1984).

[28] R. H. Busey, H. F. Holmes, and R. E. Mesmer, "The enthalpy of dilution of aqueous sodium chloride to 673 K using a new heat-flow and liquid-flow microcalorimeter. Excess thermodynamic properties and their pressure coefficients," J. Chem. Thermodyn. **16**, 343–372 (1984).

[29] D. G. Archer, "Thermodynamic properties of the NaCl + H_2O system. II. Thermodynamic properties of NaCl(aq), NaCl·$2H_2O$(cr), and phase equilibria," J. Phys. Chem. Ref. Data **21**, 793–829 (1992).

[30] R. N. Goldberg and R. L. Nuttall, "Evaluated activity and osmotic coefficients for aqueous solutions: The alkaline earth metal halides," J. Phys. Chem. Ref. Data **7**, 263–310 (1978).

[31] P. Wang, K. S. Pitzer, and J. M. Simonson, "Thermodynamic properties of aqueous magnesium chloride solutions from 250 to 600 K and to 100 MPa," J. Phys. Chem. Ref. Data **27**, 971–991 (1998).

[32] C. Christov, "Chemical equilibrium model of solution behavior and bishofite ($MgCl_2$·$6H_2O$(cr)) and hydrogen-carnallite (HCl·$MgCl_2$·$7H_2O$(cr)) solubility in the $MgCl_2$ + H_2O and HCl–$MgCl_2$ + H_2O systems to high acid concentration at (0–100) °C," J. Chem. Eng. Data **54**, 2599–2608 (2009).

[33] R. D. Lanier, "Activity coefficients of sodium chloride in aqueous three-component solutions by cation-sensitive glass electrodes," J. Phys. Chem. **69**, 3992–3998 (1965).

[34] N. Kurnakov and S. F. Zemcuzny, "Equilibria in the reciprocal system sodium chloride-magnesium sulfate with particular reference to natural brines," Z. Anorg. Allg. Chem. **140**, 149–182 (1924).

[35] S. Takegami, "Reciprocal salt pairs: $Na_2Cl_2 + MgSO_4$ and $Na_2SO_4 + MgCl_2$ at 25 °C," Mem. Coll. Sci., Univ. Kyoto, Ser. A: Math. **4**, 317–342 (1921).

[36] G. Wilczek-Vera and J. H. Vera, "On the measurement of individual ion activities," Fluid Phase Equilib. **236**, 96–110 (2005).

[37] G. Wilczek-Vera, E. Rodil, and J. H. Vera, "A complete discussion of the rationale supporting the experimental determination of individual ionic activities," Fluid Phase Equilib. **244**, 33–45 (2006).

[38] G. Wilczek-Vera and J. H. Vera, "Peculiarities of the thermodynamics of electrolyte solutions: A critical discussion," Can. J. Chem. Eng. **81**, 70–79 (2003).

[39] G. Wilczek-Vera and J. H. Vera, "The activity of individual ions. A conceptual discussion of the relation between the theory and the experimentally measured values," Fluid Phase Equilib. **312**, 79–84 (2011).

[40] G. Wilczek-Vera and J. H. Vera, "How much do we know about the activity of individual ions?," J. Chem. Thermodyn. **99**, 65–69 (2016).

[41] D. Fraenkel, "Simplified electrostatic model for the thermodynamic excess potentials of binary strong electrolyte solutions with size-dissimilar ions," Mol. Phys. **108**, 1435 (2010).

[42] D. Bashford and D. A. Case, "Generalized born models of macromolecular solvation effects," Annu. Rev. Phys. Chem. **51**, 129 (2000).

[43] W. W. Rudolph and G. Irmer, "Hydration of the calcium(II) ion in an aqueous solution of common anions (ClO_4^-, Cl^-, Br^-, and NO_3^-)," Dalton Trans. **42**, 3919 (2013).

[44] J. Mähler and I. Persson, "A study of the hydration of the alkali metal ions in aqueous solution," Inorg. Chem. **51**, 425 (2011).

[45] B. Eisenberg, "Life's solutions are complex fluids. A mathematical challenge," e-print arXiv:1207.4737 (2012).

[46] C. D. Santangelo, "Computing counterion densities at intermediate coupling," Phys. Rev. E **73**, 041512 (2006).

[47] M. Z. Bazant, B. D. Storey, and A. A. Kornyshev, "Double layer in ionic liquids: Overscreening versus crowding," Phys. Rev. Lett. **106**, 046102 (2011).

[48] I.-L. Chern, J.-G. Liu, and W.-C. Wang, "Accurate evaluation of electrostatics for macromolecules in solution," Methods Appl. Anal. **10**, 309–328 (2003).

[49] W. Geng, S. Yu, and G. Wei, "Treatment of charge singularities in implicit solvent models," J. Chem. Phys. **127**, 114106 (2007).

[50] R. S. Dembo, S. C. Eisenstat, and T. Steihaug, "Inexact Newton methods," SIAM J. Numer. Anal. **19**, 400–408 (1982).

[51] D. P. Fernandez, A. R. H. Goodwin, E. W. Lemmon, J. L. Sengers, and R. C. Williams, "A formulation for the static permittivity of water and steam at temperatures from 238 K to 873 K at pressures up to 1200 MPa, including derivatives and Debye–Hückel coefficients," J. Phys. Chem. Ref. Data **26**, 1125–1166 (1997).

[52] S. Mao and Z. Duan, "The *P*, *V*, *T*, *x* properties of binary aqueous chloride solutions up to T = 573 K and 100 MPa," J. Chem. Thermodyn. **40**, 1046–1063 (2008).